MEDWIN PUBLISHERS
Committed to create value for Researchers

International Journal of Pharmacognosy and Chinese Medicine
ISSN: 2576-4772

Toxicity Study of Hematite (A-Fe_2O_3) Nanoparticles Synthesized from Aqueous Flower Extract of *Butea Monosperma* on MCF-7 Human Breast Cancer Cell Line

Debasish P[1]*, Bandana B[2], Shakti P[2] and Adyasa S[2]

[1]Department of Pharmacy Science, Creighton University, USA

[2]University Department of Pharmaceutical Sciences, Utkal University, India

***Corresponding author:** Debasish Pradhan, Department of Pharmacy Science, Creighton University, Omaha, USA; Email: deba_udps@yahoo.co.in

Research Article

Volume 4 Issue 1

Received Date: December 10, 2019

Published Date: January 03, 2020

DOI: 10.23880/ipcm-16000193

Abstract

Background: Nanoparticles (Hematite (α-Fe_2O_3)) have been used as an antimicrobial and disinfectant agent. Nevertheless, there is limited data about antitumor potential. This study has focused on investigating cytotoxic effects of Hematite (α-Fe_2O_3) from *Butea monosperma* flower extract on MCF-7 breast cancer cells and its mechanism of action.

Materials and Methods: Thus, a green method was created for the synthesis of Hematite (α-Fe_2O_3) using an aqueous extract of *B.monosperma* flower. Synthesis of Hematite (α-Fe_2O_3) was described by different analytical techniques including ultraviolet-visible spectrophotometer, field-emission scanning electron microscopy, X-ray diffraction, and Fourier transforms infrared spectroscopy. Cell viability was determined by the 3-[4, 5-dimethylthiazol-2-yl]-a 2, 5-diphenyltetrazolium bromide assay. Reactive oxygen species (ROS) formation was measured using probe 2', 7'-dichlorofluorescein diacetate and intracellular calcium (Cai^{2+}) was evaluated with probe flu3-AM. Cells were treated with different concentrations of Hematite (α-Fe_2O_3) (1, 3, 6, 10, 15, 25, 50, and 100 μg/mL).

Results: The results showed that Hematite (α-Fe_2O_3) hindered cell growth in a dose-dependent manner. Hematite (α-Fe_2O_3) appeared to have dose-dependent cytotoxicity against MCF-7 cells through activation of the ROS generation and an increase in the intracellular Cai^{2+} (IC_{50} 52 ± 3.14).

Conclusion: The results of this preliminary study demonstrated that Hematite (α-Fe_2O_3) from *B monosperma* flower extract may be a potential therapeutic potential medicament for human breast cancer treatment.

Keywords: Biosynthesis; Cytotoxicity; MCF-7 Cell Line; *Butea Monosperma*; Iron oxide Nanoparticles

Introduction

Breast cancer is the most widely recognized reason for tumor-related death in women worldwide, and its frequency has expanded in the most recent decades [1]. It is, therefore, important to introduce new potential strategies for improving the efficacy of current cancer treatments [2,3]. Hence, introducing a biocompatible and affordable technique for treatment of cancer is imperative. Nanomedicine formulations are nanometer-sized carrier materials designed to enhance the bioavailability of the drug tissue and thus improve the treatment of chemotherapeutic drugs that are used systematically. Nanomedicine is a new approach to deliver the pharmaceuticals with safer and more effective treatments compared to conventional approaches across different route of administration [4].

Hematite (α-Fe_2O_3) has been among the most commonly used nanomaterials in our health-care system for hundreds of years. Recently, Hematite (α-Fe_2O_3) has become of intense interest in biomedical applications, because of their antibacterial, antifungal, antiviral, and anti-inflammatory activity. Among the biological techniques, (for example, use of enzymes, microorganisms, and plant extracts), the synthesis of Hematite (α-Fe_2O_3) using plant extracts is the best option for accessible traditional chemical and physical techniques [5,6]. Synthesis of plant extract nanoparticles with the help of hematite (α-Fe_2O_3) have a great impact on targeting the cells with relation to its environment safety, and simply scaled up for great range production [7]. Cytotoxic chemotherapy is a well-established treatment option for all subtypes of breast cancers, for example, doxorubicin, cisplatin, and also bleomycin [8,9]. Even though the use of doxorubicin, cisplatin, or bleomycin gives useful impact, the sufficiency and negative marks are unverifiable [10]. In this way, it is important to discover novel restorative administrators against malignancy, which are biocompatible and practical.

Natural products have been used in traditional medicine as a source of remedies for thousands of years [11]. The *Fabaceae* is a family of flowering plants, which is widely distributed in both deciduous and coniferous forests of central Europe, central Asia, North America, and especially in the Mediterranean area and is represented by about 3000 species and 220 genera [12]. Some species of the family have been used since ancient times in traditional medicine to treat eczema, wounds, goiter, ulcers, cancer, and fistulae. In addition, *Fabaceae* species have been known to be rich in glycosides [13]. In another study, the components of this plant, including cinnamic acid, three flavonoids (quercetin, isorhamnetin-3-O-rutinoside, and nepitrin) and one phenylpropanoid glycoside (acteoside 1) have been identified [14]. It has been indicated that both leaves and seeds of *Butea monosperma* contain both anticancer and cell growth enhancing agents [15]. However, the extract of this plant species, that is, *B. Monosperma* has never been examined against MCF-7 cell line. Thus, this study intended to synthesize Hematite (α-Fe_2O_3) using the natural framework and to assess potential cytotoxicity and its general mechanisms of action of biologically synthesized Hematite (α-Fe_2O_3) from *B. monosperma* in human breast cancer cells.

Materials and Methods

Preparation of Plant Extract

The flowers of *B. monosperma* were collected from the Western Mountains in Ilam Province, Iran, during April and May 2015. A voucher specimen 24998 was deposited at the Herbarium Department of the Medicinal Plants Research Center of Shiraz University. The flowers of *B. monosperma* were washed thoroughly with deionized water. About 10 g of the flowers were added to 100 mL of deionized water and boiled for 15 min in a water bath. The mixture was then filtered with Whatman filter paper grade 42. The filtered extract was stored in a refrigerator at 4°C. This extract was used as a reducing as well as a stabilizing agent [15].

Preparation of Nanoparticles Synthesized from *Butea Monosperma*

In a typical experiment, for biosynthesis of Hematite (α-Fe_2O_3), 60 mL of aqueous plant extract *B. monosperma* 10% (10 mL extract and 90 mL deionized water) was mixed with 40 mL $Fe_2O_3NO_3$ solution (0.01 M) in 250 mL Erlenmeyer flask. The flask was incubated for 24 h at 27°C at 120 rpm (Rota max 120, HeiDolph, Germany). A small aliquot of the solutions was used for the ultraviolet-visible (UV-Vis) spectroscopy. After 24 h incubation time, the reaction mixture was centrifuged at 14,000 rpm (Vision Scientific co.) for 15 min and the pellet was resuspended in a small amount of deionized water and then a small amount of suspension was sprayed on a glass slide. The resulting sediment was dried at room temperature and was used for further analyses by field-emission scanning electron microscopy (FESEM), X-ray diffraction (XRD), and Fourier transform infrared

spectroscopy (FTIR). When silver salt is treated with extract of *B monosperma* flower, the silver salt is reduced to Hematite (α-Fe_2O_3). Formation of Hematite (α-Fe_2O_3) from *B monosperma* was confirmed by UV-Vis spectral analysis. The bioreduction of $Fe_2O_3^+$ ions to Hematite (α-Fe_2O_3) was monitored by UV-Vis spectrophotometer (Rayleigh, UV-2100, China), having a resolution of 1 nm. The UV-Vis spectra were recorded using a glass cell with deionized water as a reference [16].

Field-Emission Scanning Electron Microscopy Analysis

FESEM analysis was performed using a Hitachi S4160 instrument [Japan]. Thin films of the samples were prepared on graphite adhesives. Then, the surface of the samples was coated with gold powder using a sputter hummer instrument [17].

X-Ray Diffraction Analysis

XRD analyses of the synthesized Hematite (α-Fe_2O_3) from *B monosperma* were conducted using a Bruker diffractometer (D8 Advance, Germany). The X-ray beam was Ni-filtered CuKα radiation from a sealed tube [18].

Fourier Transforms Infrared Spectroscopy Analysis

The synthesized Hematite (α-Fe_2O_3) from *B monosperma* was also analyzed by FTIR spectroscopy (Bruker Optics Ft Tensor 27, Germany) using KBr discs. The spectra were recorded in the range of 4000–400/cm [19]. Cell culture the MCF-7 (human breast carcinoma) cell line was purchased from National Cell Bank of Iran (NCBI C135). Cells were cultured in Dulbecco's modified eagle's medium (DMEM) (GIBCO, USA) supplemented with 1.5 g/L sodium bicarbonate, 10% fetal bovine serum (GIBCO, USA), 100 U/mL of penicillin, and 100 µg/mL of streptomycin (GIBCO, USA) in 25 cm^2 tissue culture flasks at 37°C in a humidified atmosphere of 5% CO_2. Cells were fed every 2–3 days and subcultured as soon as they reached a confluence of 70%–80%.

5-Dimethylthiazol-2-Yl]- A 2,5- Diphenyl tetrazolium Bromide Assay

The cell viability test was measured using the MTT color reduction test which was performed to determine the cytotoxic effect of the Hematite (α-Fe_2O_3) synthesized from *B monosperma* at different concentrations 1, 3, 6, 10, 15, 25, 50, and 100 µg/mL. The exposure time of cells with different concentrations mentioned above was 48 h. After this treatment, the MTT protocol was implemented. This method is based on the ability to survive cells to metabolize yellow tetrazolium salt MTT to purple formazan crystals by mitochondrial dehydrogenases. About 10 µL of MTT reagent (5 mg/mL) was added to 100 µL of the serum-free culture medium in each well of a 96 well plate, and after 4-h incubation, the medium was removed, and 15 µL dimethyl sulfoxide (DMSO) was added to solubilize the formazan formed by the mitochondrial reductase activity in the viable cells, Absorbance was measured at 570 nm using a microplate reader (Biotek - Elx USA). The percentFe2O3e of cell viability was calculated according to the following formula: % cell viability = ([OD treated cell − OD blank]/[OD control cell − OD blank]) × 100 [20].

Measurement of Reactive Oxygen Species

Intracellular ROS levels were detected by the fluorescent probe 2′, 7′-dichlorofluorescein diacetate (DCFH2-DA) (Sigma). In this way, 1 mL stock 10 µM prepared in DMSO added to each plate and incubated for 30 min at 37°C. Then, samples measured with fluorescent plate reader (Biotek- FL × 800). DCF fluorescence was assessed at 485 nm excitation and 520 nm emissions. ROS production was determined from an H_2O_2 standard curve (10–200 nM) [21].

Intracellular Calcium Assay

Intracellular calcium (Cai^{2+}) of MCF-7 was specified using Ca^{2+} fluorescent probe flu3-AM (Sigma) [22]. Briefly, aliquots of 1-mL MCF-7 suspensions (1 × 10^6 cells/mL) were washed with buffer A (Phenol red-free DMEM comprising 10-mM HEPES [4-[2-hydroxyethyl] piperazine-1-ethanesulfonic acid, pH 7.0) and resuspended in 200 µL of buffer A. Then, 0.4 µL of fluo 3-AM (1.0M in DMSO) was added. Cells were incubated at room temperature for 30 min and washed with buffer B (DMEM containing 10 mM HEPES, 5% fetal calf serum, and pH 7.4) before assay. Flow cytometric analysis of MCF-7 Cai^{2+} was carried out using a FACscan Calibur™ flow cytometer (Becton Dickinson, California, USA) [20].

Result

Statistical Analysis

Results are illustrated as mean ± standard deviation. Measurable assessment of the data was performed with Student's *t*-test for simple comparison between two values when suitable. For multiple comparisons, data were analyzed by analysis of variance. $P < 0.05$ was considered

statistically significant. Term half maximal inhibitory concentration (IC_{50}) refers to the toxicant concentration that induces a response halfway between the baseline and maximum after a given time of exposure.

Extracellular Synthesis of Nanoparticles Synthesized from *Butea Monosperma*

The reduction of silver ions into hematite (α-Fe_2O_3) during exposure to *B monosperma* flower extracts could be monitored by the color change. The fresh extract of *B monosperma* was yellow in color. However, after addition of $Fe_2O_3NO_3$ and incubation for 24 h, the mixture turned dark brown, which indicated the formation of Hematite (α-Fe_2O_3) (Figure 1). The color changes in aqueous solutions are due to the surface plasmon resonance (SPR) phenomenon [23]. The chemical constituents present in the plant extract play as reducing agents for the bioreduction of Fe_2O_3 ions as well as stabilizing agents.

Figure 1: The color change of Butea monosperma flower extracts before and after synthesis of nanoparticles. (a) The flower extract of Butea monosperma (yellow) and (b) Fe2O3- Butea monosperma emulsion after 24hr (reddish brown).

Ultraviolet-Visible Analysis

The formation and stability of hematite (α-Fe_2O_3) in colloidal solutions were confirmed using UV-Vis spectral analysis. The UV-Vis spectrum of biosynthesized Hematite (α-Fe_2O_3) of optimized conditions (10% extract concentration, 1:1.5 concentration ratios of the reactants, and time of 24 h) is shown in Figure 2.

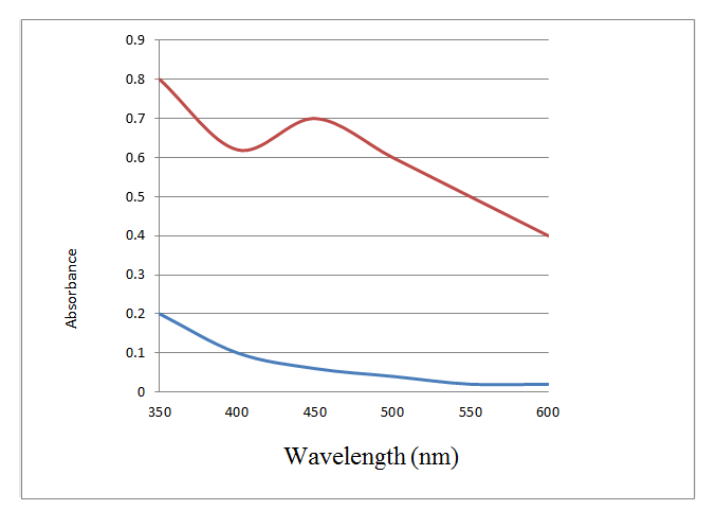

Figure 2: The ultraviolet- visible spectrum of biosynthesized nanoparticles in optimized conditions (10% extract concentration, 1:1.5 concentration ratios of the reactants, and time of 24hr).

According to the (Figure 2), the peak at 440 nm is corresponding to the SPR band of hematite (α-Fe_2O_3). The above-mentioned optimal conditions are derived from previous experience [16].

Field-Emission Scanning Electron Microscopy Analysis

The FESEM Fe_2O_3 of the biosynthesized Hematite (α-Fe_2O_3) from *B.monosperma* in optimized conditions (10% extract concentration, 1:1.5 concentration ratios of the reactants, and time of 24 h) is shown in Figure 3. According to the FESEM Fe_2O_3, the particle shape of plant-mediated Hematite (α-Fe_2O_3) was mostly spherical. The checking of FESEM Fe_2O_3 shows the faint thin layer of other material on the surface of Hematite (α-Fe_2O_3) because the extract could be played as capping Fe_2O_3 as well as a reducing agent. Since it was very difficult to measure the particle size using FESEM, all the reported particle sizes in this paper are derived from the XRD results. The purpose of the SEM method was to obtain the geometric shape of the nanoparticles. Since our synthesis is a biological synthesis, the shape of the particle should be spherical as shown in SEM (Figure 3). If our synthesis was a chemical type, their shape should be triangular.

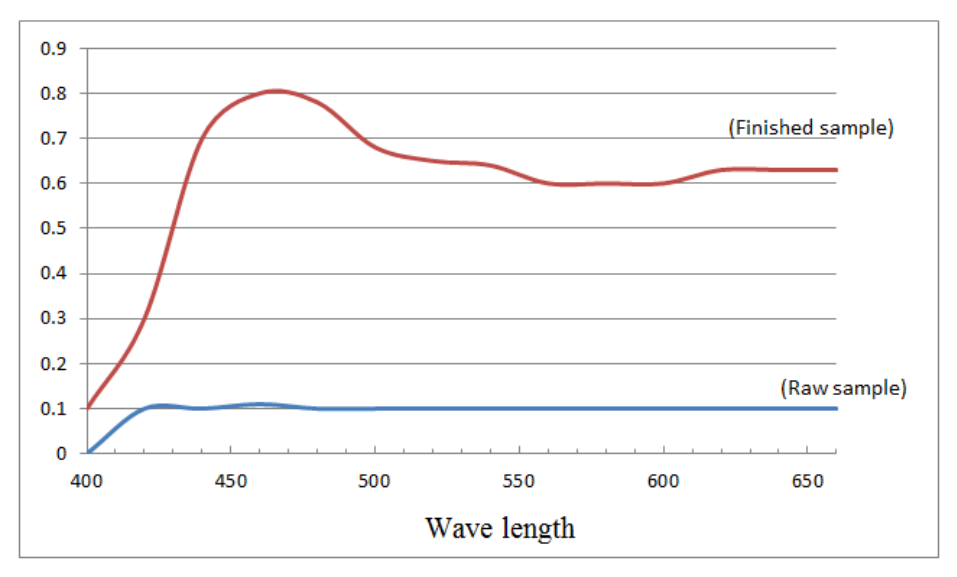

Figure 3: The field emission scanning electron microscopy Fe_2O_3 of the green synthesized nanoparticles by reduction of aqueous Fe_2O_3 ions using *Butea monosperma* flower extract under the optimized conditions.

X-Ray Diffraction Analysis

The crystalline structure of hematite (α-Fe_2O_3) was characterized using XRD analysis. (Figure 4) shows the XRD patterns of the biosynthesized Hematite (α-Fe_2O_3) from *B. monosperma*. The diffraction peak values at 2θ of 38.12°, 44.35°, 64.56°, and 77.48° correspond to lattice planes at (111), (200), (220), and (311), respectively. The XRD pattern also indicates the face-centered cubic structure of metallic Fe_2O_3. The particle size of Fe_2O_3 could be calculated by the Scherrer Equation (1): $D = 0.94\lambda/(\beta \cos \theta)$; where D is the average crystallite size, θ is the diffraction angle, β is the full width at half maximum (FWHM), and λ is the X-ray wavelength. The average crystallite size of Hematite (α-Fe_2O_3) was calculated by Equation (1) and was found to be in the range of 8–12 nm (Table 1).

According to the Fe_2O_3 of XRD, several couriers have been obtained that after transferring them to the formulas of the "Scherrer equation" numbers shown in the table. After the transferring of the obtained numbers, the nanoparticle size is obtained at about 10 nm.

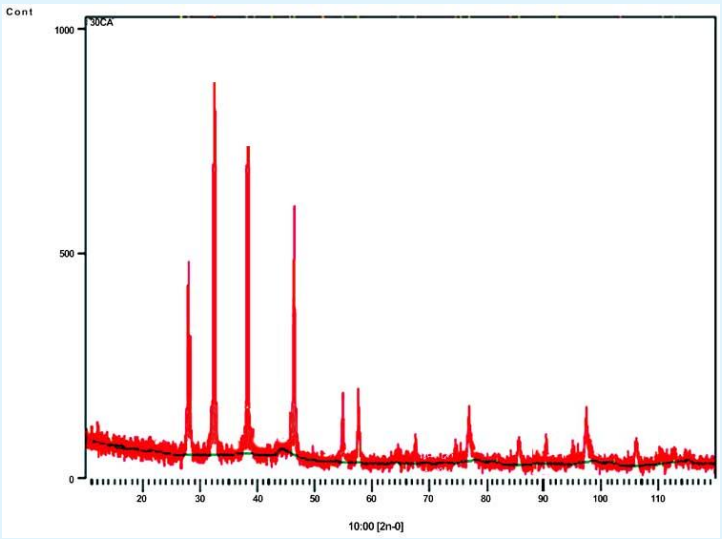

Figure 4: The X-ray diffraction pattern of biosynthesized nanoparticles from *Butea monosperma* flower extract.

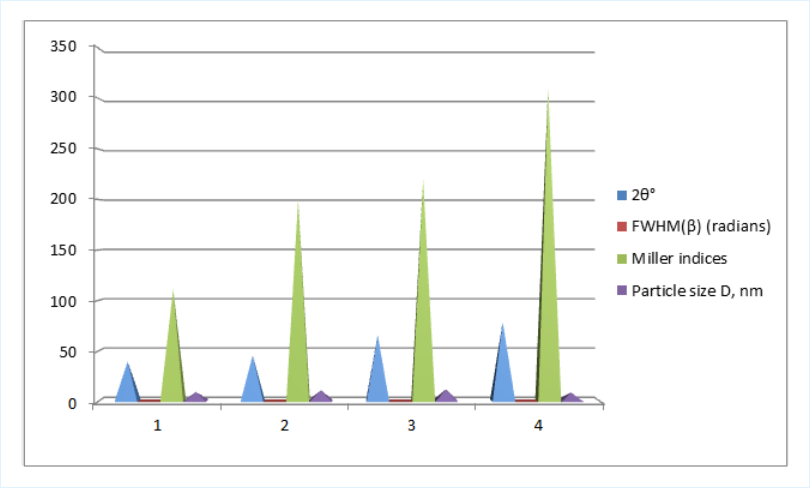

Table 1: Calculation of the average particle size of biosynthesized nanoparticles from *Butea monosperma* by Scherrer equation.

Fourier Transforms Infrared Spectroscopy Analysis

The FTIR spectrum of biosynthesized Hematite (α-Fe_2O_3) using *B monosperma* flower extract is shown in Figure 5. The spectrum shows important bands at 3454, 2255, 1650, 1480, and 1199/cm. The strong peak at 1199/cm corresponds to the C–N stretching vibration of the amine. The peak at 1480/cm can be associated with the stretching vibration C–O [–C–OH]. Strong, intense peak at 1650/cm is attributed to the C=O stretching vibration. In addition, a broad peak at 3454/cm is assigned to an O–H stretching frequency indicating the presence of hydroxyl groups. These couriers may show the ingredients in the plant extract. The FTIR analysis suggested the presence of hydroxyl, amine, and carbonyl groups in the plant extract, which may have been responsible for the reduction and/or capping and stabilization of Hematite (α-Fe_2O_3).

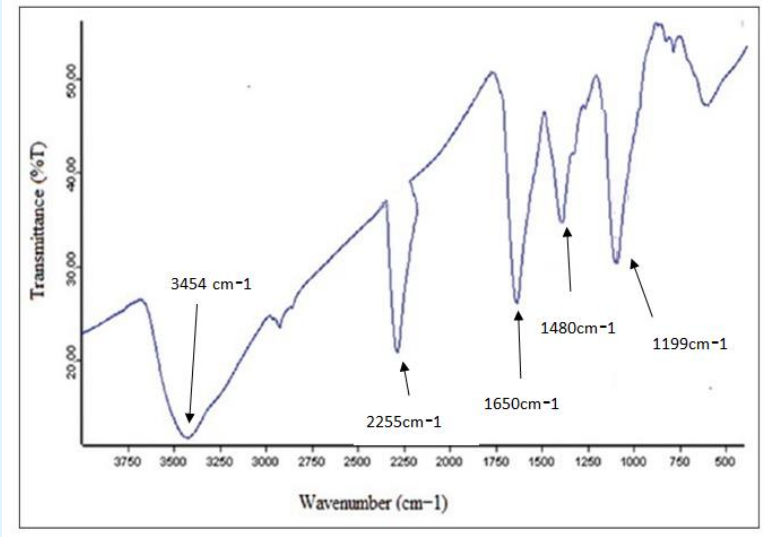

Figure 5: The FTIR spectrum of biosynthesized nanoparticles from *Buteae monosperma* flower extract.

The Cytotoxic Effects of Nanoparticles Synthesized From *Butea Monosperma* on MCF-7 Cells

The effect of hematite (α-Fe_2O_3) on the viability of MCF-7 cells was checked using the MTT assay. The hematite (α-Fe_2O_3) was able to reduce the viability of the MCF-7 cells in a concentration-dependent manner as shown in Figure 6. The anticancer activity of concentrations at 1, 3, 6, 10, 15, 25, 50, and 100 µg/mL of the synthesized Hematite (α-Fe_2O_3) from *B. monosperma* were evaluated *in vitro* against MCF-7 breast cancer cell lines after 48 h. hematite (α-Fe_2O_3) at concentrations 25, 50 ($P < 0.05$ vs. control), and 100 µg/mL increased cell death ($P < 0.001$ vs. control). However, plant extract did not. The effect of different concentrations of Hematite (α-Fe_2O_3) was tested on MCF-7 cells. Incubation with hematite (α-Fe_2O_3) synthesized from *B monosperma* at high concentrations, that is, 25, 50, and 100 µg/mL, led to a reduction in cell viability with IC_{50} value of 52 ± 3.14 µg/mL.

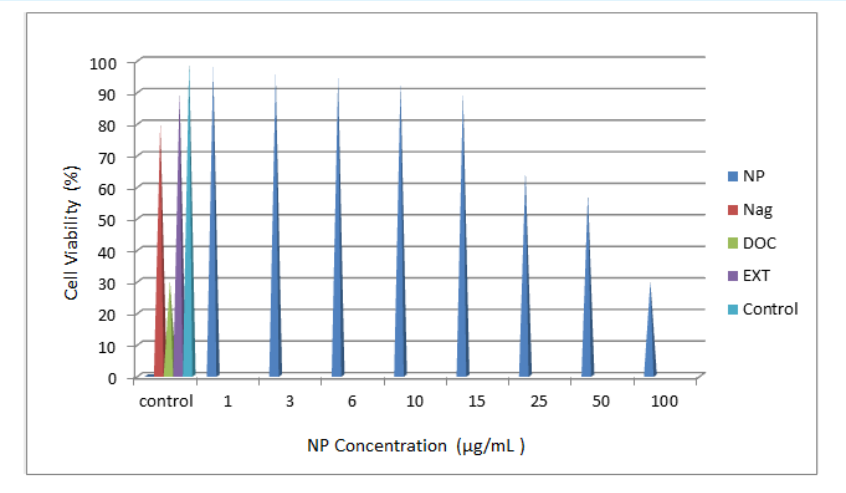

Figure 6: Effect of nanoparticles synthesized from Butea monosperma cell viability of MCF-7 cells.

Cells were treated with nanoparticles at various concentrations for 48h and cytotoxicity was determined by the MTT method. Nanoparticles from Butea monosperma flower extract [NP], $Fe_2O_3NO_3$ [NFe_2O_3] (0.01 M), docetaxel [DOC] (120 nM), and Extract [EXT] (100 µg/ml). *P < 0.05 versus control, **P < 0.001 versus control. Since the main objective of this study was to investigate the diversity of biological nanoparticles, extract "EXT," nanoparticles "NFe_2O_3," and docetaxel "DOC" were used as controls and the concentration variation in them was not important for this study.

Effect of Nanoparticles Synthesized from *Butea Monosperma* on Reactive Oxygen Species Generation

Our experiments provided evidence for a molecular mechanism of the Fe_2O_3 NP-inducing generation of ROS, and it could be one of the factors for apoptosis. To know the effect of Hematite (α-Fe_2O_3) in oxidative stress, measured ROS generation using the H2 DCF-DA assay. Hematite (α-Fe_2O_3) induced intracellular ROS generation was evaluated using intracellular peroxide-dependent oxidation of DCFH2-DA to form fluorescent DCF. DCF fluorescence was detected in cells treated with Hematite (α-Fe_2O_3) for 48 h. As shown in Figure 7, the ROS levels generated in response to Hematite (α-Fe_2O_3) were significantly higher in Hematite (α-Fe_2O_3)-treated cells than control. Taken together, all these results indicate that cell death is mediated by ROS production, which might alter the cellular redox status, and it is a potential reason for cell death. The Hematite (α-Fe_2O_3) at concentration 25, 50 (P < 0.05 vs. control) and 100 µg/mL (P < 0.001 vs. control) significantly induced the intracellular ROS production in MCF-7 cells. Treatment with N-acetyl-L-cysteine (5 mM) prevented the enhancement of DCF fluorescence intensity.

Relatively fluorescence of 2', 7'-dichlorofluorescein diacetate was measured at 485 nm excitation and 520 nm emissions. N-acetyl-L-cysteine [NAC] (5mM), hematite treated cells [HTC], docetaxel [DOC] (120 nM), and extract [EXT] (100µg/ml). *P < 0.05 versus control, **P < 0.001 versus control.

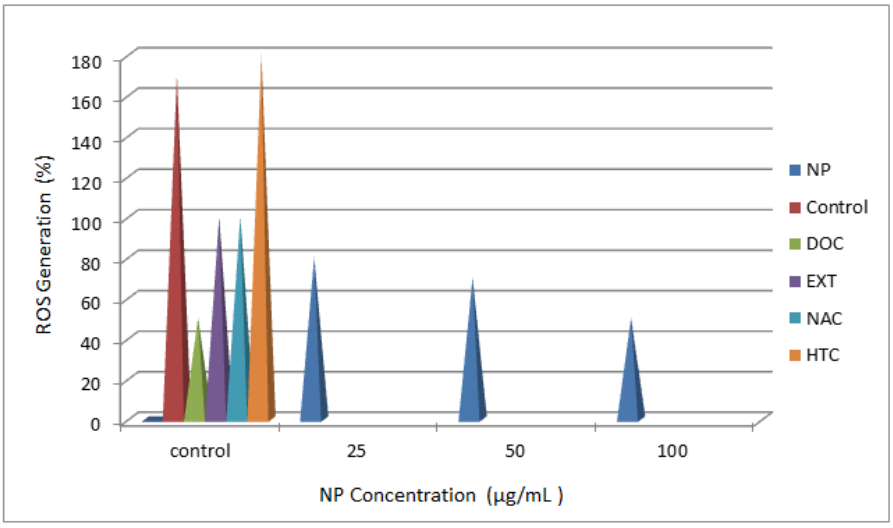

Figure 7: Reactive oxygen species generation in nanoparticles synthesized from *Butea monosperma* treated MCF-7 cells.

Effect of Nanoparticles Synthesized from *Butea Monosperma*on Cai^{2+}

The effect of different concentrations of Hematite (α-Fe_2O_3) was tested on MCF-7 cells (Figure 8). Hematite (α-Fe_2O_3) synthesized from *B monosperma* increased intracellular of Cai^{2+} at concentrations 25, 50 ($P < 0.05$ vs. control) and 100 µg/mL ($P < 0.001$ vs. control); however, plant extract did not. (Fe_2NO_3) (0.01 M) increased intracellular of Cai^{2+} ($P < 0.05$ vs. control).

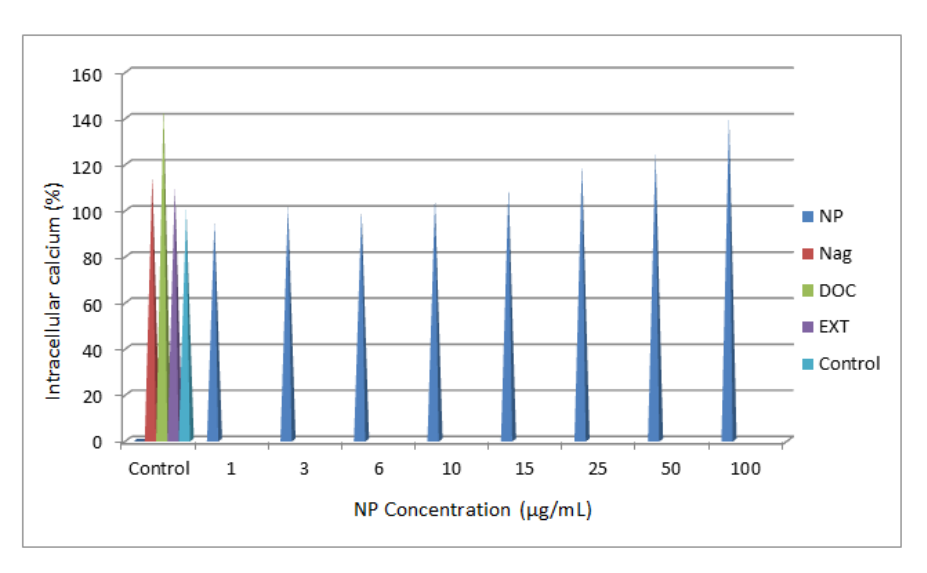

Figure 8: Effect of nanoparticles synthesized from *Butea monospermaon* intracellular of calcium (Ca^{2+}). Increases in Ca^{2+} levels and cytotoxicity after 48hr were often linked. $Fe_2O_3NO_3$ [NFe_2O_3] (0.01 M), docetaxel [DOC] (120nM), and extract [EXT] (100µg/ml). *P < 0.05 versus control, **P < 0.001 versus control.

Discussion

Overall, our results showed that the biologically synthesized hematite (α-Fe_2O_3) has antiproliferative activity through induction of cell death in MCF-7 breast cancer cell line, proposing that biologically synthesized Hematite (α-Fe_2O_3) might be a potential option specialist for human breast cancer therapy. Hematite (α-Fe_2O_3) are metallic nanostructures with useful surface properties and have been used for various purposes, such as the production of wound dressings and cosmetics and in the medical industry as device-coating agents [24,25]. However, many studies showed that Hematite (α-Fe_2O_3) may induce genotoxicity and cytotoxicity in cancer and normal cell lines [24]. Physical and chemical properties of Hematite (α-Fe_2O_3), including surface chemistry, weight, size distribution, shape, particle morphology, particle composition, coating/capping, agglomeration, dissolution rate, solution particle reactivity, efficiency of ion release, type of cell, and finally type of reducing agents used for synthesis, are essential elements in determining cytotoxicity [25]. In the present study, the phytochemicals present in the extract of *B monosperma* flower are, namely glycosides and flavonoids, which act as reducing as well as a capping agent and helping in stabilizing the nanoparticles. In the phytochemical analysis of the flowers of *B. monosperma* proteins, flavonoids, terpenoids, cardoacglycoside and tannins, etc., plays a more fundamental role in biobased nanoparticles synthesis. This synthesized nanoparticles show the optical properties and tailorability for applications having capping and reducing agent. Since the plant components are flavonoids, some of the effects observed in this study are likely to be reflected in this component. It has already been observed that quercetin in the plant has been effective on MCF-7 cells by increasing cell death, reducing cell proliferation, and effecting free radicals [26]. When silver salt is treated with an extract of *B monosperma* flower, the silver salt is reduced to Hematite (α-Fe_2O_3). The synthesized nanoparticles, which are capped with *B monosperma* extract also, exhibit enhanced anticancer activity. In the present study, the UV-Vis results showed a peak at 440 nm corresponding to the SPR in the optimized conditions (10% extract concentration, 1:1.5 concentration ratios of the reactants and time of 24 h). To obtain the optimized conditions for synthesis of Hematite (α-Fe_2O_3), the effect of process variables such as extract concentration, the concentration ratio of the reactants and time was studied using UV-Vis spectroscopy. In this assessment, the reduction of silver ions into Hematite (α-Fe_2O_3) during exposure to *B.monosperma* flower extracts could be monitored by the color change. The fresh extract of *B.monosperma* was yellow in color. However, after addition of $Fe_2O_3NO_3$ and incubation for 24 h, the mixture

turned dark brown, which indicated the formation of Hematite (α-Fe_2O_3). It seems that the color changes in aqueous solutions are due to the SPR phenomenon [27]. The chemical constituents present in *B.monosperma* flower extract play as reducing agents for the bioreduction of Fe_2O_3 ions as well as stabilizing agents. The UV-Vis spectrum of hematite (α-Fe_2O_3) in aqueous solution shows an absorbance peak around 450 nm due to SPR [28,29]. Our results showed that the SEM Fe_2O_3 of Hematite (α-Fe_2O_3) were spherical. In another study, the SEM Fe_2O_3 showed relatively spherical-shaped particles in the range of 30–50 nm [30]. XRD pattern also clearly showed that the Hematite (α-Fe_2O_3) formed by the reduction of Fe_2O_3+ ions by the *B monosperma* flower extract are crystalline in nature [31]. The FTIR spectrum showed the presence of various functional groups like hydroxyl groups, amine groups and carbonyl groups. Indeed, FTIR spectroscopy measurements are carried out to identify the biomolecules that bound specifically on the silver surface and the local molecular environment of capping agent on the nanoparticles. The FTIR spectroscopic study confirmed that the guava extract has the ability to perform both reduction and capping functions on the Hematite (α-Fe_2O_3) [32]. In another study, the FTIR peak at 1637/cm for Hematite (α-Fe_2O_3) synthesized using *Andrographis paniculata* extracts can be attributed to the carbonyl stretch of amides and could be associated to proteins that potentially cap Hematite (α-Fe_2O_3) [33].

The cell viability assay is an important method for cytotoxicity analysis that describes the cellular response to toxic materials and it can provide information on cell death, survival, and metabolic activities [34]. In our experiment, results suggest that Hematite (α-Fe_2O_3) were able to reduce the cell viability of MCF-7 cells in a do se-dependent manner in MCF-7 cells for 48 hr. Hematite (α-Fe_2O_3) synthesized from *B.monosperma* at high concentration concentrations (25, 50, and 100 µg/mL) increased cell death with an IC_{50} value of 52 ± 3.14 µg/mL. Nevertheless, plant extract at 2 mg/mL did not exhibit any cell death. It has been reported that the IC_{50} value against A549 cells was 40 µg/mL for Hematite (α-Fe_2O_3) synthesized by extracts of *Gossypium hirsutum* [34]. Our results suggest that the highest concentration of Hematite (α-Fe_2O_3) synthesized from *B.monosperma* significantly inhibits the growth of cells. It has been reported that Hematite (α-Fe_2O_3) and $Fe_2O_3NO_3$ have cytotoxicity in a dose-dependent manner in human Chang liver cells, among these materials Hematite (α-Fe_2O_3) showed higher cytotoxicity compared to $Fe_2O_3NO_3$ [35]. Moreover, Hematite (α-Fe_2O_3)-treated cells showed the decreased metabolic activity, which depends on nature of cell types and size of nanoparticles [35]. The cytotoxic activity of the synthesized Hematite (α-Fe_2O_3) extract containing Hematite (α-Fe_2O_3) has been investigated against human breast cancer cell (MCF-7) and the IC_{50} were found to be 50 ± 0.04 µg/mL at 24 h. Although the synthesized nanoparticles from the *B.monosperma* in this study have reduced cell viability in MCF-7 human breast cancer cell line, it may also affect the normal cells in the body. In the present study, the potentiality of Hematite (α-Fe_2O3) synthesized from *B.monosperma* to induce oxidative stress was assessed by measuring the intracellular ROS level. MCF-7 cells exposed to Hematite (α-Fe_2O_3) for 48 h showed increased ROS formation as evidenced by the increased DCF fluorescence intensity. The Hematite (α-Fe_2O_3) from *B.monosperma* significantly induced intracellular ROS production in MCF-7 cells at the concentrations 25, 50, and 100 µg/mL. Elevated levels of ROS due to Fe_2O_3 NPs exposure may lead to the failure of cellular antioxidant defense system in MCF-7 cells and thereby severe oxidative attack. Oxidative stress is one of the key mechanisms of toxicity related to nanoparticle exposure [32]. ROS generation has been shown to play an important role in apoptosis induced by treatment with Hematite (α-Fe_2O_3) [20nm] [36-39]. The toxicity was evaluated using changes in cell morphology, cell viability, metabolic activity, and oxidative stress [40]. In another study, smaller particles of Hematite (α-Fe_2O_3) with a size 15 nm hydrocarbon-coated are reported to produce more toxicity in macrophages Fe_2O_3 than the size 55 nm by increasing the ROS generation [41]. Interestingly, hematite (α-Fe_2O_3) themselves can produce ROS and oxidative stress as well as the process to release Fe_2O_3+ [42]. Nevertheless, it has been concluded that increased levels of oxidative stress markers and decreased levels of antioxidants in carcinoma suggest that oxidative stress markers play a significant role in pathophysiology of this cancer [43]. The effect of ROS on cancer cells is controversial. The extent of ROS-induced damage can be exacerbated by decreased efficiency of antioxidant defense mechanisms. Antioxidants have been shown to inhibit initiation and promotion in carcinogenesis and counteract cell immortalization and transformation [44]. It has been observed that diets rich in fruits and vegetables can decrease both oxidative DNA damage and cancer incidence. By contrast, agents increasing oxidative DNA damage usually increase the risk of developing cancer [45]. Understanding the role of ROS at the molecular level is very important for designing a suitable protective strategy for cancer treatment, which has attracted the attention of researchers.

Hematite (α-Fe_2O_3) synthesized from *B.monosperma* increased Cai^{2+} at concentrations 25, 50, and 100 µg/mL in a dose-depended manner in MCF-7 cells although plant extract (only one concentration was used) did not. Cai^{2+} is believed to play a crucial role in mediating cell death. An increased amount of Cai^{2+} causes more mitochondrial Ca^{2+} uptake. Ca^{2+} accumulation in mitochondria is one of the primary causes of mitochondrial permeability transition (PT), through the opening of the PT-pore, and this is an important key factor in the apoptotic pathway [46]. It has been reported that TiO_2, Fe_2O_3, ZnONPs and quantum dots increase intracellular calcium by releasing calcium from intracellular stores and facilitating the entry of calcium into the cell [47]. Changes in Cai^{2+} levels mediate a variety of cellular processes. High Cai^{2+} levels mediate plasma membrane repair but may also induce cell death [48,49]. Although there was no clear link between increased Cai^{2+} levels and lysosomal dame or ROS generation in MCF-7 cells, they both were increased cell death in a dose-dependent manner.

Conclusion

Hematites (α-Fe_2O_3) have emerged as an important class of nanomaterials for a wide range of industrial and medical applications. Developing biocompatible molecule, using nanotechnology, as an anticancer agent is one of the novel approaches in the field of cancer therapy. We have successfully synthesized and prepared stable Hematite (α-Fe_2O_3) (8-12 nm) using an aqueous extract of *B.monosperma* flower, which is environmentally friendly, cost-effective, and rapid method for synthesis of Hematite (α-Fe_2O_3). Hence, this study focused on the cytotoxicity assay of Hematite (α-Fe_2O_3) from *B.monosperma* on MCF-7 breast cancer cells and its mechanism of cell death. We observed that Hematite (α-Fe_2O_3) from *B.monosperma* hindered the growth of MCF-7 breast cancer cells in a dose-dependent manner using the MTT test. It appeared to exert cytotoxic activity through activation of the ROS generation and Cai^{2+} increase. The present results demonstrated that Hematite (α-Fe_2O_3) from *B.monosperma* may be a potential therapeutic medicament for human breast cancer treatment.

Acknowledgement: The authors are thankful to DST Inspire and ICMR, New Delhi for their research grant.

Conflict of Interest

Authors are only responsible for article content. Authors did not have any conflicts of interest.

References

1. Sulaiman SF, Najimuddin N, Samian MR, Muhammad TS (2005) Methanolic extract of Pereskia bleo (Kunth) DC. (Cactaceae) induces apoptosis in breast carcinoma, T47-D cell line. J Ethnopharmacol 96(1-2): 287-294.

2. Jemal A, Siegel R, Xu J, Ward E (2010) Cancer statistics, 2010. CA Cancer J Clin 60(5): 277-300.

3. Pradhan D, Joshi V, Tripathy G (2010) Anticancer effect of S Trifoliatus on human breast cancer cell lines. IJPBS 1(1): 1-9.

4. Matei A, Cernica I, Cadar O, Roman C, Schiopu V (2008) Synthesis and characterization of ZnO-Polymer nanocomposites. Int J Mater Form 1(1): 767-770.

5. Prakash Rao S, Pradhan D (2012) Protective Potential of Flucourtiaindica Ulcer Inventi Impact. Ethnopharmacology 1(1): 21-214.

6. Vigneshwaran N, Ashtaputre NM, Varadarajan PV, Nachane RP, Paralikar KM, et al. (2007) Biological synthesis of silver nanoparticles using the fungus Aspergillus flavus. Mater Lett 61(6): 1413-1418.

7. Zhu SL, Palchik O, Koltypin Y, Gedanken A (2000) Shape-controlled synthesis of silver nanoparticles by pulse sonoelectrochemical methods. Langmuir 16(16): 6396-6399.

8. Kim D, Jeong S, Moon J (2006) Synthesis of silver nanoparticles using the polyol process and the influence of precursor injection. Nanotechnology 17(16): 4019-4024.

9. Mittal AK, Chisti Y, Banerjee UC (2013) Synthesis of metallic nanoparticles using plant extracts. Biotechnol Adv 31(2): 346-356.

10. Pradhan S, Mohapatra R, Pradhan D (2015) Ethnomedicinal plants of Odisha used against Breast Cancer-A review. IJCPRR 1(2): 38-42.

11. Richman A, Broothaerts W, Kohn J (1997) Self-incompatibility RNases from three plant families: Homology or convergence? Am J Bot 84(7): 912.

12. Park SU, Park NI, Kim YK, Suh SY, Eom SH, et al. (2009) Application of plant biotechnology in the medicinal plant, Rehmannia glutinosa Liboschitz. Med Plants Res 3(13): 1258-1263.

13. Ardeshiry Lajimi A, Rezaie Tavirani M, Mortazavi SA, Barzegar M, Moghadamnia SH, et al. (2010) Study of anti-cancer property of Scrophularia striata extract on the human astrocytoma cell line (1321). Iran J Pharm Res 9(4): 403-410.

14. Prashant T, Susmita J, Pratap Kumar S (2019) Butea Monosperma: Phytochemistry and Pharmacology. Acta Scientific Pharmaceutical Sciences 3(4): 19-26.

15. Ghaffari Moghaddam M, Hadi Dabanlou R (2014) Plant mediated green synthesis and antibacterial activity of silver nanoparticles using Crataegus douglasii fruit extract. J Ind Eng Chem 20(2): 739-744.

16. Mameneh R, Ghaffari Moghaddam M, Solouki M, Samzadeh Kermani A, Sharifmoghadam MR (2015) Characterization and antibacterial activity of plant mediated silver nanoparticles biosynthesized using Scrophularia striata flower extract. Russ J Appl Chem 88: 538-546.

17. Geethalakshmi R, Sarada DV (2012) Gold and silver nanoparticles from Trianthema decandra: Synthesis, characterization, and antimicrobial properties. Int J Nanomedicine 7: 5375-5384.

18. Pradhan S, Pradhan D, Behera B (2018) Antiproliferation activity of Ocimumgratissimum aqueous extract on human breast cancer MCF-7 cell line. WJPR 7(9): 421-428.

19. Karuppiah M, Rajmohan R (2013) Green synthesis of silver nanoparticles using Ixora coccinea leaves extract. Mater Lett 97: 141-143.

20. Sladowski D, Steer SJ, Clothier RH, Balls M (1993) An improved MTT assay. J Immunol Methods 157(1-2): 203-207.

21. Zhu H, He M, Bannenberg GL, Moldéus P, Shertzer HG (1996) Effects of glutathione and pH on the oxidation of biomarkers of cellular oxidative stress. Arch Toxicol 70(10): 628-634.

22. Abbasi N, Akhavan MM, Rahbar Roshandel N, Shafiei M (2014) The effects of low and high concentrations of luteolin on cultured human endothelial cells under normal and glucotoxic conditions: Involvement of integrin-linked kinase and cyclooxygenase-2. Phytother Res 28(9): 1301-1307.

23. Mason SV, Misra IM, Mohanty AK (2012) Switchgrass Panicum virgatum extract mediated green synthesis of silver nanoparticles. Nano Sci Eng 2(2): 47-52.

24.

25. Susan WP, Wijnhoven WJ, Carla A, Werner IH, Agnes GO, et al. (2009) Nano silver a review of available data and knowledge gaps in human and environmental risk assessment. Nanotoxicology 3(2):109-138.

26. Pradhan D, Tripathy G, Pradhan RK, Pradhan S, Dasmohapatra T (2016) A Review on cuminosides nanomedicine-Pharmacognostic approach to cancer therapeutics. JYP(PUBMED) 8(2): 61-71.

27. Davatgaran Taghipour Y, Masoomzadeh S, Farzaei MH, Bahramsoltani R, Karimi Soureh Z, et al. (2017) Polyphenol nanoformulations for cancer therapy: Experimental evidence and clinical perspective. Int J Nanomedicine 12: 2689-26702.

28. Yoon KY, Hoon Byeon J, Park JH, Hwang J (2007) Susceptibility constants of escherichia coli and bacillus subtilis to silver and copper nanoparticles. Sci Total Environ 373(2-3): 572-575.

29. Jignasu P Mehta, Balubhai A, Golakiya (2014) Determination of flavonoids, phenolic acid and polyalcoholic in Butea Monosperma and Hedychium coronarium by semipreparative HPLC photo diode array (PDA) detector. Arabian Journal of Chemistry 7(6): 1110-1115.

30. Amel Hanini, Alain Schmitt, Kamel Kacem, François Chau, Souad Ammar, et al. (2011) Evaluation of iron oxide nanoparticle biocompatibility. Int J Nanomedicine 6: 787-794.

31. Ghaffari Moghaddam M, Hadi Dabanlou R, Khajeh M, Rakhshanipour M, Shameli K (2014) Green synthesis of silver nanoparticles using plant extracts. Korean J Chem Eng 31: 548-557.

32. Supraja SM, Chakravarthy N, Priya AJ, Sagadevan E, Kasinathan MK, et al. (2013) Green synthesis of silver nanoparticles from Cynodon dactylon leaf extract. Chem Tech Res 5(1): 271-277.

33. Yang X, Li Q, Wang H, Huang J, Lin L, et al. (2010) Green synthesis of palladium nanoparticles using broth of Cinnamomum camphora leaf. J Nanopart Res 12(5): 1589-1598.

34. Ren Y, Yang H, Wang T, Wang C (2016) Green synthesis and antimicrobial activity of monodisperse silver nanoparticles synthesized using Ginkgo biloba leaf extract. Phys Lett A 380(45): 3773-3777.

35. Pradhan D, Panda PK, Tripathy G (2009) Hepatoprotective.....CCL4 hepatotoxic rats. Adv Pharmacol Toxicol 10(1): 43-48.

36. Kanipandian N, Thirumurugan R (2014) A feasible approach to phyto-mediated synthesis of silver nanoparticles using industrial crop Gossypium hirsutum (cotton) extract as stabilizing agent and assessment of its in vitro biomedical potential. Ind Crop Prod 55: 1-10.

37. Romeilah RM (2009) Anticancer and antioxidant activities of Matricaria chamomilla L. and Marjorana hortensis essential oils. Res J Med Med Sci 4: 332-339.

38. Asha Rani PV, Low Kah Mun G, Hande MP, Valiyaveettil S (2009) Cytotoxicity and genotoxicity of silver nanoparticles in human cells. ACS Nano 3(2): 279-2790.

39. Park MV, Neigh AM, Vermeulen JP, de la Fonteyne LJ, Verharen HW, et al. (2011) The effect of particle size on the cytotoxicity, inflammation, developmental toxicity and genotoxicity of silver nanoparticles. Biomaterials 32(36): 9810-9817.

40. Piao MJ, Kang KA, Lee IK, Kim HS, Kim S, et al. (2011) Silver nanoparticles induce oxidative cell damage in human liver cells through inhibition of reduced glutathione and induction of mitochondria-involved apoptosis. Toxicol Lett 201(1): 92-100.

41. Reddy NJ, Nagoor Vali D, Rani M, Rani SS (2014) Evaluation of antioxidant, antibacterial and cytotoxic effects of green synthesized silver nanoparticles by Piper longum fruit. Mater Sci Eng C Mater Biol Appl 34: 115-122.

42. Carlson C, Hussain SM, Schrand AM, Braydich Stolle LK, Hess KL, et al. (2008) Unique cellular interaction of silver nanoparticles: Size-dependent generation of reactive oxygen species. J Phys Chem B 112(43): 13608-13619.

43. Kawata K, Osawa M, Okabe S (2009) In vitro toxicity of silver nanoparticles at noncytotoxic doses to hepG2 human hepatoma cells. Environ Sci Technol 43(15): 6046-6051.

44. Badjatia N, Satyam A, Singh P, Seth A, Sharma A (2010) Altered antioxidant status and lipid peroxidation in Indian patients with urothelial bladder carcinoma. Urol Oncol 28(4): 360-367.

45. Matés JM, Pérez Gómez C, Núñez de Castro I (1999) Antioxidant enzymes and human diseases. Clin Biochem 32(8): 595-603.

46. Halliwell B (2002) Effect of diet on cancer development: Is oxidative DNA damage a biomarker? Free Radic Biol Med 32(10): 968-974.

47. Jeyaraj M, Sathishkumar G, Sivanandhan G, MubarakAli D, Rajesh M, et al. (2013) Biogenic silver nanoparticles for cancer treatment: An experimental report. Colloids Surf B Biointerfaces 106: 86-92.

48. Huang da W, Sherman BT, Lempicki RA (2009) Systematic and integrative analysis of large gene lists using DAVID bioinformatics resources. Nat Protoc 4(1): 44-57.

49. Gitanjali Tripathy, Debasish Pradhan (2013) Evaluation of in-vitro immunomodulatory activity of Beta vulgaris. AJPCR, pp: 370-377.

50. Ujwala ST, Amul Rao UB, Jyotsna SM (2017) Tailor able optical properties of silver nanoparticles from Butea Monosperma plant extract 2(4): 189-194.